

Supplemental Information

Computational Fluid Dynamics Simulations (CFD)

The liquid jet formation in a microfluidic liquid jet device is simulated using COMSOL Multiphysics v4.2a. The tasks for CFD-simulations involve the creation of the 3D-geometry, the setup of the fluid model, mesh generation and the analysis of the results, as illustrated in Fig. S1.

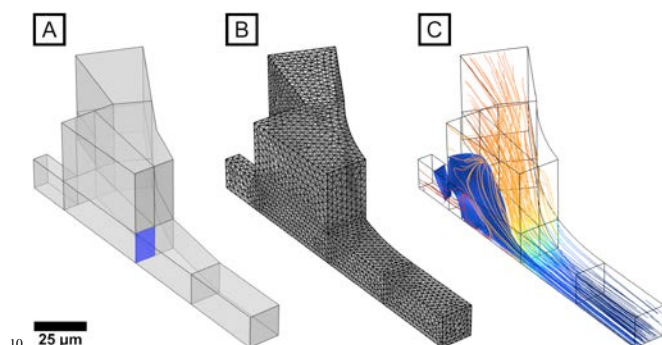


Fig. S1 Towards the simulation of the fluid flow inside the microfluidic liquid jet device: (A) Import of the 3D device geometry drawn in AutoCAD 2013 (the blue square marks the initial liquid-gas interface) (B) mesh generation and (C) solution of the model. The scale bar denotes 25 μm .

First, the CAD-designed geometry of the microfluidic liquid jet device is imported into COMSOL. This file contains exactly the same geometric design which was used for the photo mask of the soft lithographic fabrication process. Thereafter, the boundary conditions are assigned to the microchannel walls, to the inlets and the outlet of the device assuming time-dependent conditions and finite elements are generated based on this geometry. To describe the interplay of describes air and water, we chose a two-phase model which is based on the level-set method.^{S1,S2} Using this model, we performed the simulation for the Newtonian fluid water and the underlying fluid dynamics are described by the incompressible Navier-Stokes equations:

$$\rho \frac{\partial \mathbf{u}}{\partial t} + \rho (\mathbf{u} \cdot \nabla) \mathbf{u} = \nabla \cdot \left[-p \mathbf{I} + \mu (\nabla \mathbf{u} + \nabla \mathbf{u}^T) \right] + \mathbf{F}_g + \mathbf{F}_{st} + \mathbf{F}_{ext} + \mathbf{F}$$

$$\nabla \cdot \mathbf{u} = 0$$

with the density of the fluid ρ , the pressure p , the identity matrix \mathbf{I} , the dynamic viscosity of the fluid μ , the velocity field \mathbf{u} and the different forces \mathbf{F} (gravity (g), surface tension (st), external free energy (ext), volume (no index)).

The movement of the fluid-fluid interface of the two-phase flow within the velocity field are described by the mentioned level set method which is based on the following formulas.

$$\frac{\partial \phi}{\partial t} + \mathbf{u} \cdot \nabla \phi = \gamma \nabla \cdot \left(\varepsilon \nabla \phi - \phi (1 - \phi) \frac{\nabla \phi}{|\nabla \phi|} \right)$$

$$\rho = \rho_1 + (\rho_2 - \rho_1) \phi$$

$$\mu = \mu_1 + (\mu_2 - \mu_1) \phi$$

The parameter ε determines the thickness of the region where ϕ goes smoothly from zero to one and is typically of the same order as the size of the elements of the mesh. ε is constant within each domain and equals the largest value of the mesh size h within the domain. The parameter γ determines the amount of reinitialization or stabilization of the level set function. The constant densities of fluid 1 and 2 are described by ρ_1 and ρ_2 and their dynamic viscosities by μ_1 and μ_2 , respectively. Here, fluid 1 corresponds to the domain where $\phi < 0.5$, and fluid 2 corresponds to the domain where $\phi > 0.5$.

The 3D model is solved for 77223 finite elements and 402905 degrees of freedom. The average element quality of the mesh is 0.7659 on a scale from 0 to 1, where 1 is the highest quality. All relevant constants that are used in the simulations are summarized in Tab. S1.

Tab. S1 Material properties used in the simulation model.

Parameter	Value
flow speed v ($\mu\text{L h}^{-1}$)	600
flow speed v (m s^{-1})	0.37037
main channel height h_{MC} (μm)	30
main channel width w_{MC} (μm)	15
temperature T (K)	293.15
pressure difference Δp_g (bar)	0.25
surface tension water/air σ (N m^{-1}) ^{S3}	0.0782
viscosity η ($\text{kg} \cdot \text{m}^{-1} \text{s}^{-1}$) ^{S4}	
time frame t (μs)	0 to 750

Gas flow rate analysis

The gas flow rate is analyzed to quantify the vacuum compatibility of the microfluidic liquid jet devices. This task is performed by putting the microfluidic device slightly under water and measuring the time until 25 mL of gas are collected in a reservoir. The results are shown in Fig. S2 and Tab. S2. The measured gas flow rates should allow a vacuum of 10^{-6} bar at a (high, but reasonable) vacuum pumping speed of 1000 l s^{-1} .

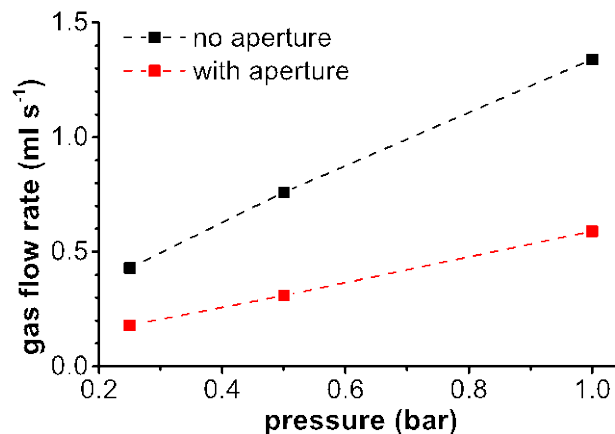


Fig. S2 Change of the gas flow rates depending on the applied pressures and on the nozzle geometry. The outlet cross section with an aperture is $30 \cdot 30 \mu\text{m}^2$ while the nozzle-less version has a cross section of $30 \cdot 90 \mu\text{m}^2$.

Tab. S2 Gas flow rates under different conditions.

p (bar)	no aperture (30-90 μm^2)	with aperture (30-30 μm^2)
	flow rate (ml s^{-1})	flow rate (ml s^{-1})
0.25	0.43	0.18
0.5	0.76	0.31
1	1.34	0.59

Jetting of protein crystallization buffers

To demonstrate the microfluidic liquid jet devices' compatibility with other liquids than pure water, the devices are operated with different solutions that are examples for commonly used protein crystallization buffers. These aqueous solutions contain high concentrations of poly(ethylene glycol) (PEG, $M_n = 400$ & 3350 g mol^{-1}), ammonium sulfate ($(\text{NH}_4)_2\text{SO}_4$), 2-methyl-2,4-pentanediol (MPD) (all obtained from Sigma Aldrich) and/or TacsimateTM pH 4.0. The latter is a readily-available crystallization reagent by Hampton Research and contains 1.8305 M malonic acid, 0.25 M ammonium citrate tribasic, 0.12 M succinic acid, 0.3 M DL-malic acid, 0.4 M sodium acetate trihydrate, 0.5 M sodium formate and 0.16 M ammonium tartrate dibasic.^{S5,S6}

The liquid flow rate is set to $1000 \mu\text{l h}^{-1}$ at an applied pressure of 0.5 bar and images are captured every 20 s until the experiment was *intentionally* stopped after 60 min. The microfluidic liquid jet devices operate error free and without any indication of clogging as shown in Fig. S3.

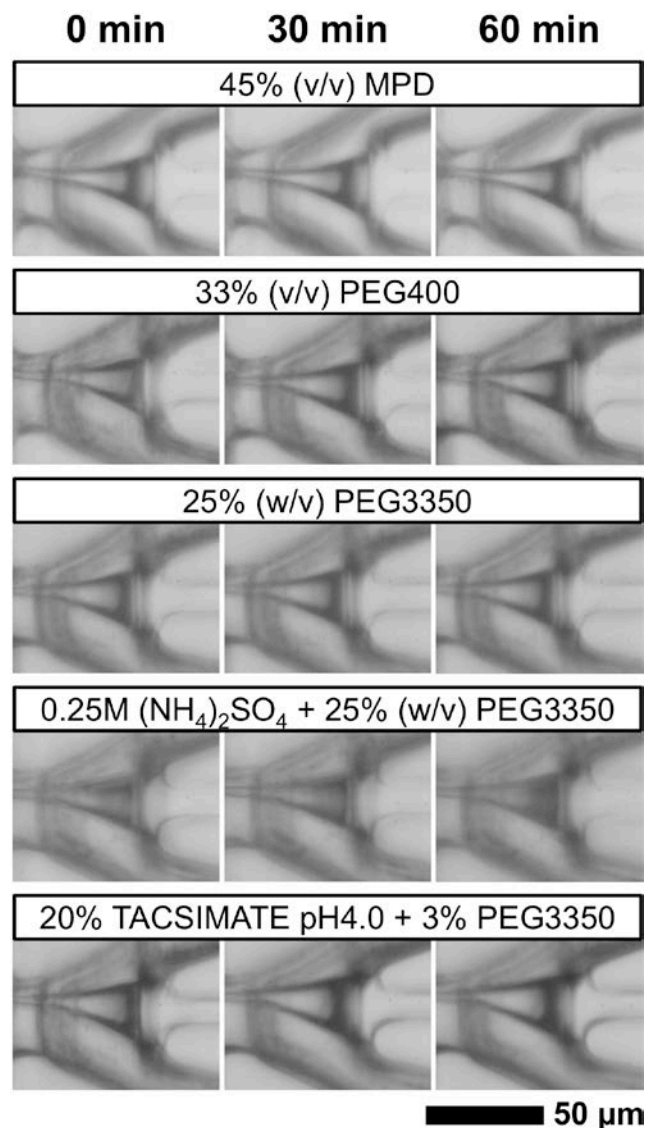


Fig. S3 Microscopic images of the microfluidic liquid jet device during operation with different solutions over extended times. These solutions are examples of commonly used protein crystallization buffers containing high concentrations of PEG and/or salts. The liquid flow rate is set to $1000 \mu\text{l h}^{-1}$ at an applied pressure of 0.5 bar.

- S1. *CFD Module User's Guide for COMSOL v4.2a*, COMSOL AB, 2011, 211-215.
- S2. E. Olsson and G. Kreiss, *J. Comput. Phys.* 2005, **210**, 225–246.
- S3. N. R. Pallas and Y. Harrison, *Colloids Surf.*, 1990, **43**, 169–194.
- S4. R. Weast, M. Astle, *Handbook of Chemistry and Physics*, 60th edition, CRC Press, Boca Raton, 1979, F-11, F-49.
- S5. Hampton Research - Production Information: What is TacsimateTM?, http://hamptonresearch.com/documents/product/hr000175_what_is_tacsimate_new.pdf, (accessed Jan 2014).
- S6. A. McPherson and B. Cudney, *J. Struct. Biol.*, 2006, **156**, 387–406.